Journal of Solar Energy Research (JSER)

Journal homepage: www.jser.ut.ac.ir

A Computational Study On the Effect of Geometrical Configurations On Axisymmetric Solar Chimney Performance

Birju Yagnik[a,*], Bharat Ramani[b]

[a]*Gujarat Technological University, Ahmedabad, Gujarat, India*
[b]*SLTIET, Gujarat Technological University, Ahmedabad, Gujarat, India*

ARTICLE INFO

Article Type:

Research Article

Received:2025.10.14
Accepted in revised form: 2025.12.20

Keywords:
Solar chimney;
Collector;
Area ratio;
Turbulence model;
Solar radiation

A B S T R A C T

This work presents a CFD-based evaluation of the airflow behavior inside a solar chimney power plant, focusing on the buoyancy forces generated when solar energy heats the air beneath the collector. An axisymmetric model inspired by the Manzanares, Spain SCPP prototype with its central updraft tower was developed and simulated in ANSYS Fluent using a finite-volume framework. The analysis uses the standard k–ε turbulence model together with the Boussinesq approximation to represent density variations under moderate temperature differences. Predicted inlet velocities and temperatures at the chimney base were compared with available experimental measurements to confirm model accuracy. A soil layer beneath the collector was included as a thermal-storage medium, which increased heat retention and helped sustain stronger airflow, producing velocities up to approximately 17.49 m/s. Parametric studies showed that enlarging both the chimney height and collector radius yielded a noticeable rise in power potential. Temperature in the tower region increased from about 300 K to nearly 379.5 K depending on the operating conditions. Additional simulations conducted at solar irradiance levels of 400 and 1000 W/m² generated inlet velocities of roughly 11 m/s and 22 m/s, respectively. Upon examined, revealing its influence on the achievable pressure difference and power output.

1. Introduction

The world's continued reliance on fossil-based energy sources such as coal, oil, and natural gas has raised significant environmental concerns, particularly with respect to greenhouse gas emissions and long-term resource depletion. Many developing regions struggle with the high cost of conventional energy infrastructure, while alternatives such as nuclear power are often considered too risky or

*Corresponding Author Email: birjuyagnik29@gmail.com

Cite this article: Yagnik, B. and Ramani, B. (2025). A Computational Study on The Effect of Geometrical Configurations on Axisymmetric Solar Chimney Performance. Journal of Solar Energy Research, 10(4), 2645-2656. doi: 10.22059/jser.2025.404298.1652

DOI: 10.22059/jser.2025.404298.1652

economically burdensome. These limitations highlight the need for renewable, low-maintenance, and regionally adaptable energy technologies.

Solar energy remains one of the most scalable and abundant renewable energy resources. Among various solar-thermal technologies, the Solar Chimney Power Plant (SCPP) represents a distinctive approach that uses natural convection to generate electricity. The concept relies on heating ambient air beneath a large, transparent collector, causing it to rise through a tall chimney. As the warm air ascends, fresh air is drawn inward from the collector perimeter, creating a continuous circulation pattern driven by buoyancy. A turbine placed within the airflow path converts this kinetic energy into mechanical power, which is subsequently transformed into electricity.

Several Dai et al. [1] investigated the potential of SCPPs in regions of northwestern China with strong solar resources. Their work highlighted the sensitivity of power output to collector diameter, chimney height, turbine efficiency, and local weather conditions. Pastohr et al. [2] performed one of the early comprehensive CFD studies of the Manzanares prototype using an axisymmetric model and a simplified treatment of solar radiation. They observed that increasing the thermal input beneath the collector enhances both velocity and temperature within the tower, underscoring the importance of accounting for unsteady heat exchange between the ground and the air.

Pretorius and Kröger [3] proposed a more refined representation of convective heat transfer inside the chimney and demonstrated that this improved formulation reduces the predicted impact of the turbine on system performance. Ming et al. [4] incorporated a thermal storage layer beneath the collector and showed that both temperature and airflow increase with rising solar radiation. Their follow-up study [5], which explicitly modeled the turbine, predicted a maximum power output of around 50 kW for the Manzanares prototype and examined how turbine rotational speed alters the chimney outlet conditions.

Several authors have focused specifically on geometric optimization. Xinping et al. [6] explored the relationship between chimney height and power generation, identifying an optimal tower height for maximum output using data from the Spanish prototype as a reference. Lorente et al. [7] approached the problem from a constructal design perspective and described how SCPP installations can be distributed over available land in a performance-efficient manner. Xu et al. [8] developed a numerical model that included both a turbine and a thermal storage layer to assess the combined impacts of solar radiation intensity and turbine-induced pressure losses. Their findings indicated that substantial energy loss occurs through the collector cover, especially under higher radiation.

Ambient wind effects on the SCPP have been investigated by Ming et al. [9], who reported that lateral winds can significantly disrupt the inlet airflow. They recommended adding a circular barrier around the collector edge to diminish this adverse influence. Li et al. [10] created a thermodynamic model validated with field data from the Manzanares plant and observed that the presence of a turbine reduces the overall power output relative to idealized unloaded conditions. They also noted that beyond a certain collector radius, further increases do not provide meaningful performance gains.

Choi et al. [11] established an analytical model for temperature distribution inside the collector and considered the use of water as a nighttime thermal storage medium. Fasel et al. [12] extended CFD analysis across a broad range of chimney heights—from laboratory scale to theoretical 1000 m structures—and identified several flow features, including convection rolls and turbulent behaviour in the chimney. Cao et al. [13] used TRNSYS to compare performance at different geographic locations and emphasized that solar irradiation plays a more dominant role than ambient temperature in determining yearly energy yield.

Beyond structural dimensions, researchers have also studied how blockages, roof geometry, and chamber shape influence airflow. Ming et al. [14] demonstrated that adding a short wall in front of the collector inlet can reduce cross-wind disturbances and improve output. Koonsrisuk and colleagues contributed several studies [15,16] examining flow-area variations, sloped collectors, and divergent chimney configurations, concluding that appropriate combinations of these geometric features can markedly improve second-law efficiency and reduce entropy generation.

Further enhancements have been proposed by Sandeep et al. [17], who used CFD to identify optimal inlet heights, chimney divergence angles, and collector outlet radii. Okada et al. [18] evaluated a diffuser-shaped chimney and showed that static-pressure recovery inside the tower can significantly elevate airflow velocity compared to a conventional cylindrical design. Gholamalizadeh et al. [19] emphasized the importance of accurately representing the greenhouse effect in numerical models, arguing that neglecting this mechanism underestimates collector temperatures.

Other studies have examined canopy profiles and radiative heat-transfer modelling. Cottam et al. [20] assessed different collector roof shapes and found that maintaining a sufficient collector height near the chimney inlet is critical for enhancing kinetic energy at the turbine location. Huang et al. [21] introduced a parallel-plate model that incorporates solar radiation inside the collector and achieved strong agreement with experimental and three-dimensional simulation data. Semai et al. [22] analyzed how canopy slope and different thermal storage materials affect entropy generation and overall system performance.

Regional evaluations of SCPPs have also been conducted. Rabehi et al. [23] simulated systems at four Algerian locations and reported monthly power outputs between 68–73 kW. Zhou et al. [24] examined the effect of varying chimney flow area on turbine pressure drop and fluid power, confirming the advantages of a divergent chimney top. Shiyang et al. [25] further evaluated chimney divergence and demonstrated significant performance gains relative to cylindrical chimneys. Xu and Zhou [26] expanded this analysis by studying the impact of chimney outlet–to–inlet area ratio, reporting a maximum predicted output of 231.7 kW at an area ratio of 8.7.

This study numerically evaluates a modified solar chimney incorporating a divergent tower and convergent collector using 3D CFD modeling. Results demonstrate a near threefold increase in power output compared with the conventional Manzanares configuration, primarily due to enhanced airflow acceleration and thermal utilization [28].

A CFD-based investigation examines how inclined absorber surfaces influence airflow and power generation in solar chimney systems. Optimization of absorber slope and central height led to a significant rise in maximum air velocity and a power enhancement exceeding 30% relative to the reference plant [29].

This work presents a three-dimensional CFD model of a solar chimney integrated with an axial turbine under realistic climatic conditions. Seasonal variations were shown to strongly affect velocity and energy production, with peak monthly electricity output occurring during high-temperature periods [30].

This comprehensive review establishes standardized CFD validation procedures for solar chimney power plants using the Manzanares prototype as a benchmark. It highlights best practices in turbulence modeling, radiation treatment, mesh independence, and boundary condition selection for reliable numerical predictions [31].

This study explores the integration of ground-based waste heat sources into a solar chimney system using 3D CFD simulations. The results indicate that supplemental heat significantly improves power output, even in low or zero solar radiation conditions, enabling near-continuous operation [32].

Despite extensive research on individual parameters, relatively fewer studies have examined the combined influence of geometric configuration, solar radiation intensity, and chimney shape on SCPP power production. The present study aims to address this gap by evaluating how chimney height, collector diameter, solar radiation, and chimney convergence collectively affect the overall performance of an SCPP modelled after the Manzanares prototype.

2. Materials and Methods

Data obtained from the Manzanares prototype indicates that the plant's power output (Pt) can be estimated using a thermodynamic analysis of the solar chimney system, as described by Fasel et al. (2013).

$$P_t = \eta_c h \eta_c \frac{2}{3} g \frac{H\, ch\, \pi R^2 I}{CT} \qquad (1)$$

Total in this context, ηch and ηc represent the efficiencies of the chimney and the collector, respectively; g is the gravitational acceleration, *Hch* is the height of the chimney, R denotes the radius of the collector, I refers to solar irradiance, and Ta is the ambient temperature. The solar radiation absorbed by the collector surface generates natural convection within the Solar Chimney Power Plant (SCPP). The Rayleigh number (Ra) is employed to quantify the buoyancy-driven flow strength of the fluid inside the chimney.

$$R_a = \frac{g\beta \Delta T L^3}{av} \qquad (2)$$

In this study, ΔT denotes the peak temperature variation within the SCPP, L is the height at the collector's inlet, β represents thermal diffusivity, α is the thermal expansion coefficient, and g refers to gravitational acceleration. The calculated Rayleigh number in this analysis exceeds 1010, which is indicative of the shift from laminar to turbulent convective flow. As a result, turbulence modeling has been incorporated into the simulation to accurately capture the fluid behavior inside the SCPP. Figure 1 illustrates the schematic layout of the SCPP system. The primary governing equations—namely continuity, momentum, energy, and the standard k-ε

turbulence model—are solved using numerical methods.

The boundary conditions used in the current simulation of the Solar Chimney Power Plant (SCPP) are summarized in Table 1. The chimney wall is modeled as adiabatic, implying no heat transfer occurs through its surface. A constant temperature boundary is applied to the ground. Additionally, a cylindrical soil region with a radius of 5 meters and a depth of 5 meters is included in the simulation domain. The side surfaces of the thermal energy storage layer are also treated as adiabatic, ensuring thermal insulation from surrounding elements.

An axisymmetric model of the Solar Chimney Power Plant (SCPP) has been analyzed using steady-state numerical simulations, with the turbine incorporated into the system. Since a 2D turbine model only represents the flow behavior and assumes an ideal pressure drop, it is used to characterize the flow dynamics within the plant. To evaluate the power output of the SCPP in the CFD simulation, both the velocity profile and the average airflow velocity have been calculated.

The current simulation is based on a physical model of the Manzanares solar chimney prototype in Spain, as depicted in Fig. 1. The model features a chimney structure with a height of 195 meters and a radius of 5 meters. The solar collector has a radius of 120 meters and is elevated 1.7 meters above the ground. For this simulation, the Boussinesq approximation is applied, as it is appropriate for the thermal and flow conditions under investigation.

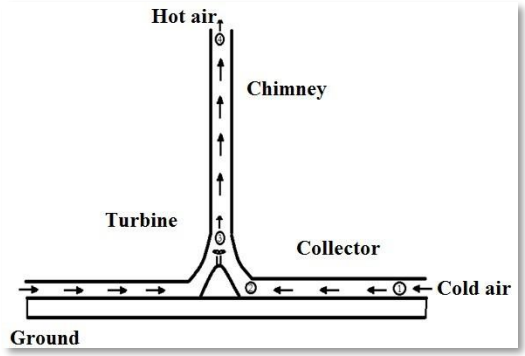

Figure 1. Schematic representation of the solar chimney power plant, illustrating the collector region, chimney structure, and ground layer

In this simulation, the continuity, Navier-Stokes, and energy equations were solved using the SIMPLE algorithm, and the computations were carried out with ANSYS Fluent. The geometrical parameters used in the analysis were taken from the Spanish SCPP prototype. To capture the airflow and heat transfer behavior within the plant, the standard k-ε two-equation turbulence model was applied, along with the standard wall function approach for near-wall regions. For modeling radiative heat transfer, the Discrete Ordinates (DO) model was selected due to its effectiveness in simulating radiation transport and its capability to account for direct solar loading. The convective and diffusive terms were discretized using a second-order accurate upwind scheme to enhance solution precision. The chimney, ground, and collector domains were meshed using quadrilateral elements. The pressure-velocity coupling was handled with the SIMPLE scheme, while the turbulence, momentum, energy, and radiation equations were also solved using a second-order upwind discretization. Spatial gradients were evaluated using the Least Squares Cell-Based method.

Table 1. Mesh statistics demonstrating adequate orthogonality and aspect ratios for numerical stability

Cells	Faces	Nodes
40838	84042	43206

Table 2. Quality metrics demonstrating adequate orthogonality and aspect ratios for numerical stability

Name	Type	Min Orthogonal	Max Aspect Ratio
Fluid	Quad	0.81478156	3.8323402
Soil	Quad	1	1.4196135

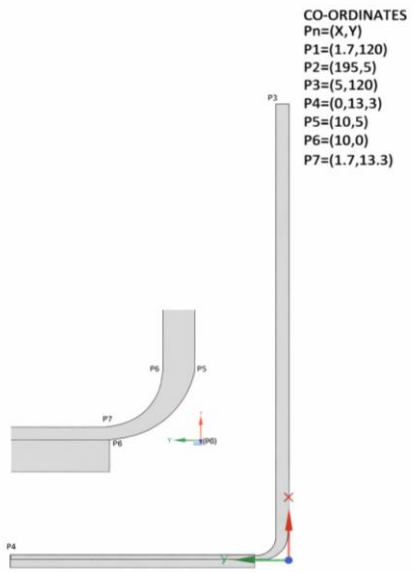

Figure 2. Geometric layout of the computational model showing the collector, chimney, and soil domains

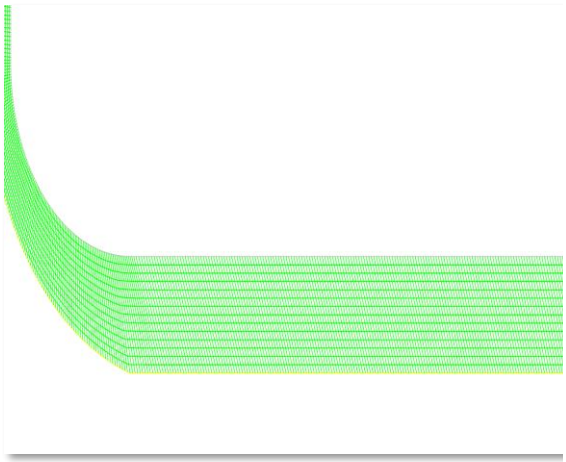

Figure 3. Mesh distribution across the collector region

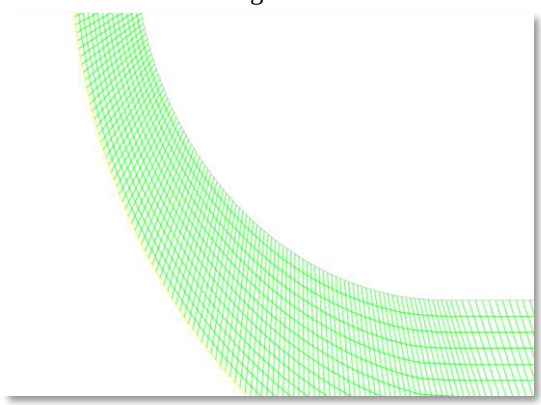

Figure 4. Mesh distribution across curvature transition

Table 3. Summary of boundary conditions applied to the computational domains, including thermal and flow constraints for each surface

Boundary	Type	Conditions
Chimney wall	Wall	Fixed heat flux
Collector	Wall	Heat Flux 8 W/m2
Ground	Wall	Fixed heat flux
Collector inlet	Pressure inlet	ΔPin= 0; Tin = Tamb
Chimney Outlet	Pressure outlet	ΔPout= 0 Tout = Tamb-0.065×Hch

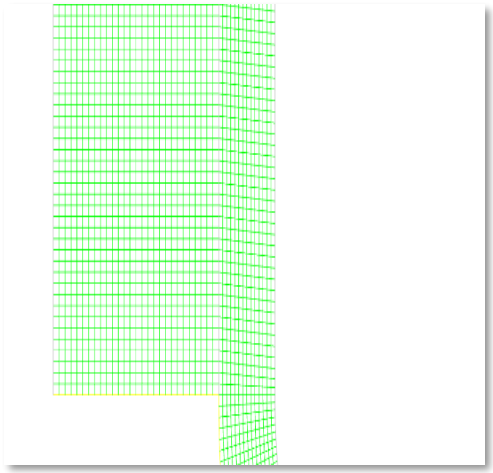

Figure 5. Mesh distribution across chimney base

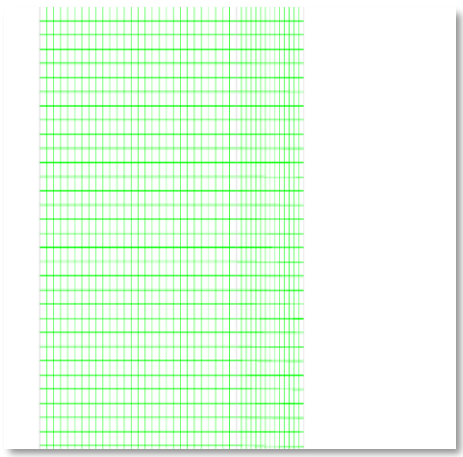

Figure 6. Mesh distribution across chimney top

3. Results and Discussion

Air velocity begins to increase significantly at the chimney inlet. Experimental observations from the Manzanares prototype (under load conditions) reported average inlet velocities in the range of 7-14 m/s, along with a maximum air temperature increase of approximately 15–20 K. Consider “Collector radius” as X Axis and “Chimney height” as Y Axis of the Figures 7, 8, 9, 11 and 12 Contour. The temperature gain within the collector is a key factor influencing the collector's thermal efficiency. Figure 7 and 8 display the velocity and temperature contour plots, respectively. According to the simulation, the average airflow velocity and the temperature increase are found to be 11 m/s and 22 K, respectively.

These values were obtained by performing an integral average over the contour plots.

The simulation results show a noticeable increase in air velocity at the chimney inlet as air flows from the collector area. The peak temperature occurs beneath the collector. Overall, the numerical findings align well with the experimental data from the Manzanares facility, indicating that the current simulation approach is quite reliable. Minor differences in predicted velocity and temperature values can be attributed to the presence of a turbine at the chimney entrance in the physical prototype, which reduces airflow speed. In contrast, the present study does not include the turbine in its model. Additionally, an axisymmetric geometry is used for the solar chimney, and some uncertainties such as variations in air density and humidity are acknowledged in the analysis.

Figures 9 illustrate the velocity profiles within the SCPP system using soil as the thermal storage medium, for solar radiation intensities of 400 W/m2. Figures 11 and 12 indicate that air velocity rises with an increase in solar radiation from 400 to 1000 W/m². The highest air velocity occurs at the chimney inlet. Specifically, peak velocities within the chimney are recorded as 11.8, 14.1, and 15.7 m/s for radiation intensities of 400, 600, and 800 W/m², respectively. Without a turbine, the maximum chimney inlet velocity can reach approximately 22.5 m/s under a solar radiation intensity of 1000 W/m². This clearly demonstrates that solar radiation significantly influences airflow velocity by raising the temperature beneath the collector, which enhances the buoyancy effect due to increased temperature-driven density differences. This, in turn, results in a pressure difference. Figure 4 shows how air velocity within the collector varies across different radiation levels. Both average and maximum velocities increase as air moves toward the chimney and as radiation intensity rises. Similarly, Figures 5 and 6 depict the distribution and variation of air temperature within the collector under different radiation intensities. Air temperature also climbs toward the chimney with higher levels of solar radiation.

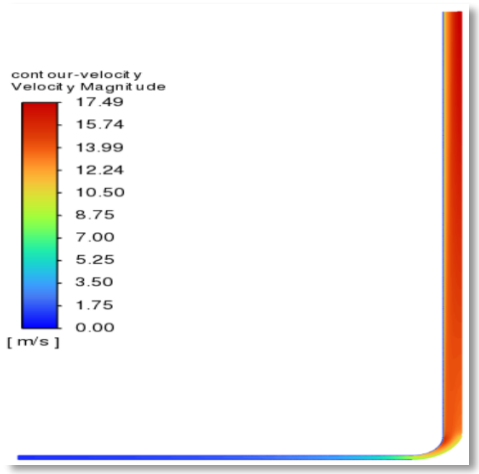

Figure 7. Velocity distribution within the collector and chimney region under the specified radiation condition, showing the general thermal buildup and transport toward the tower inlet

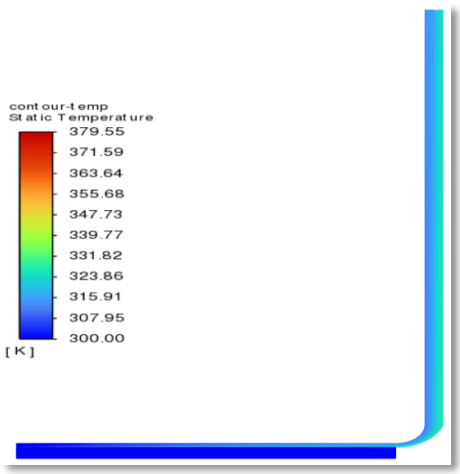

Figure 8. Static Temperature distribution within the collector and chimney region under the specified radiation condition, showing the general thermal buildup and transport toward the tower inlet

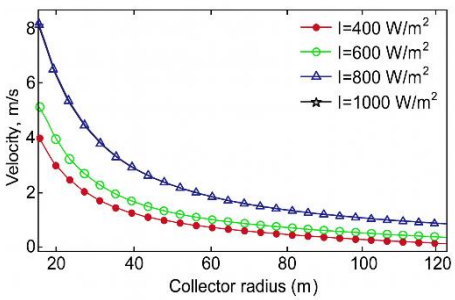

Figure 9. Airflow velocity contours illustrating the acceleration of air as it moves from the collector zone toward the chimney entrance

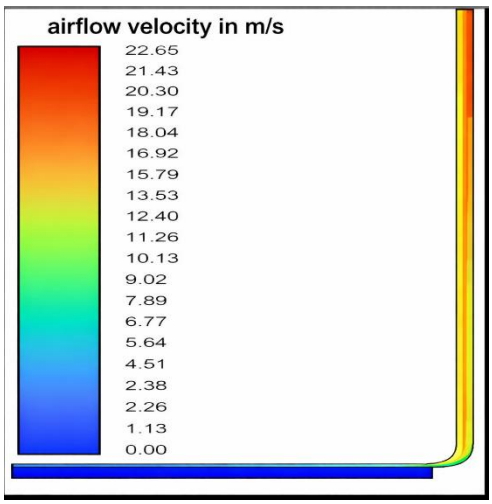

Figure 10. Comparison of velocity fields for different solar-irradiance inputs, highlighting the influence of radiation intensity on thermal uplift

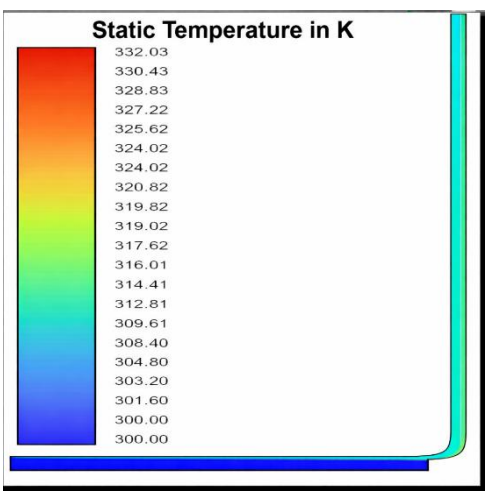

Figure 11. Temperature profiles at selected planes inside the SCPP, demonstrating changes in flow magnitude with varying radiation levels

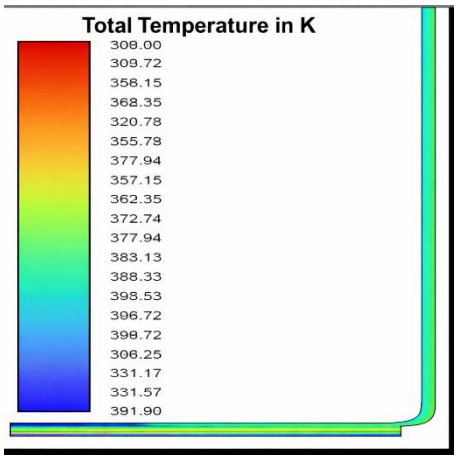

Figure 12. Temperature profiles at selected planes inside the SCPP, demonstrating changes in flow magnitude with varying radiation levels

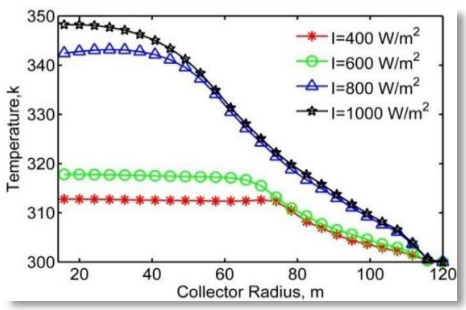

Figure 13. Comparison of temperature fields for different solar-irradiance inputs, highlighting the influence of radiation intensity on thermal uplift

The heated, low-density air generated beneath the collector roof is converted into kinetic energy as it rises through the chimney of the SCPP. Studies have indicated that, under unloaded conditions, the power output of an SCPP is directly linked to the chimney height (Reference). Within the chimney, air temperature tends to either slightly decrease or remain nearly unchanged due to the influence of gravitational potential energy.

Consequently, as chimney height increases, the buoyant force acting on the air diminishes. In this study, a modified version of the Manzanares prototype—identical in all aspects except chimney height—is analyzed under a solar radiation intensity of 1000 W/m² to assess how chimney height affects SCPP performance.

To evaluate power generation efficiency, maximum air velocity and power output have been used as performance indicators. Figures 9(a) and 9(b) depict the relationship between chimney height and air velocity, as well as power output. Since power output is directly proportional to chimney height, it is evident that increasing chimney height leads to greater power generation. However, the rate of this increase declines gradually. This diminishing return is attributed to the reduced buoyancy effect and energy losses in airflow. As shown in Figure 7(b), results based on the Manzanares prototype suggest that a chimney height of 1900 meters yields the highest power output. Beyond this height, further increases do not significantly improve performance.

According to theoretical analysis under unloaded conditions, the power output of a Solar Chimney Power Plant (SCPP) is directly proportional to the square of the collector radius, provided the chimney height remains constant. In this study, the maximum collector radius of the Manzanares prototype, as proposed in theoretical models, is used for evaluation under a solar radiation intensity of 1000 W/m². All other main dimensions of the prototype are kept unchanged, except for the collector radius. To assess performance, the maximum air velocity point is selected for each collector radius.

As depicted in Figure 11, the air velocity inside the SCPP rises noticeably as the collector radius increases, up to 320 meters. However, the rate of increase in both air velocity and power output begins to slow as the radius extends to 395 meters and eventually stabilizes beyond this point. Therefore, it can be concluded that for the Manzanares prototype, the optimal collector radius is 395 meters—beyond which further increases do not lead to significant improvements in power output. The primary factor limiting performance beyond this radius is excessive heat loss, which occurs through radiation from the roof to the sky, convection to the surrounding air, and conduction from the ground into deeper soil layers. As a result, expanding the collector radius beyond 395 meters does not enhance power output, making further enlargement economically and energetically inefficient.

This section explores how the cross-sectional shape of the chimney affects the performance of a Solar Chimney Power Plant (SCPP). To evaluate the impact of a convergent chimney design, various outlet-to-inlet area ratios were modeled and analyzed using ANSYS Fluent. Figure 10 presents the velocity profiles along the height of the chimney for different area ratios.

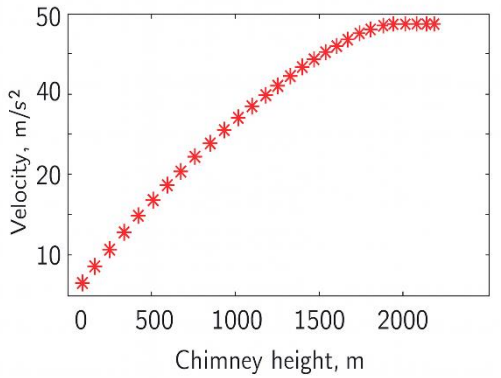

Figure 14. Variation in inlet velocity for several chimney heights, indicating how increased tower elevation alters buoyancy-driven flow

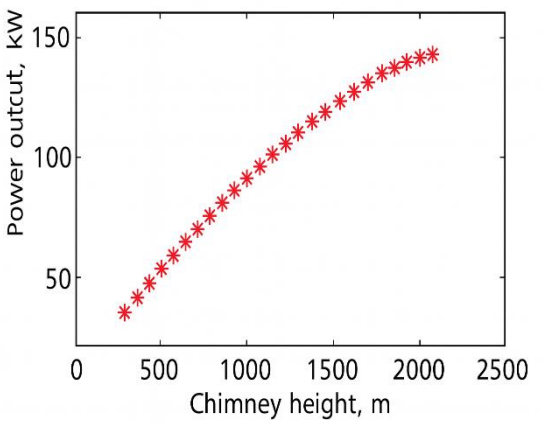

Figure 15. Estimated power output behavior along the chimney height, illustrating the impact of expanded absorber area on air heating

The analysis reveals that, regardless of the area ratio (AR), air velocity within the collector increases as it approaches the chimney inlet. However, within the chimney itself, the air velocity is influenced by the ratio of outlet to inlet area. Four different area ratios for the convergent chimney shape were examined: AR = 0.25, 0.5, 0.75, and 1.0. The Manzanares prototype, for reference, features a chimney with a uniform cross-section (AR = 1.0).

In all convergent chimney configurations where AR is less than 1, air velocity continues to rise and reaches its peak at the chimney exit. As shown in Figure 11, a lower AR results in a higher air velocity at the chimney inlet compared to a chimney with a

uniform diameter. This indicates that a convergent chimney shape can enhance airflow velocity, potentially improving the system's overall performance.

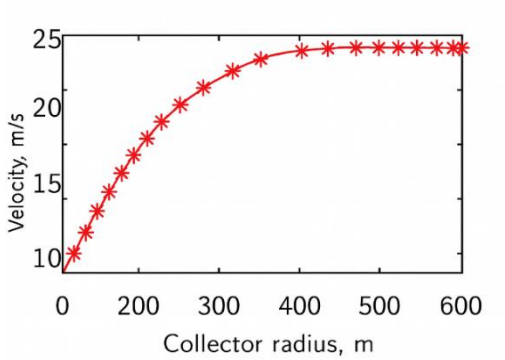

Figure 16. Velocity field comparison for divergent chimney configurations with different outlet-to-inlet area ratios, showing changes in acceleration patterns

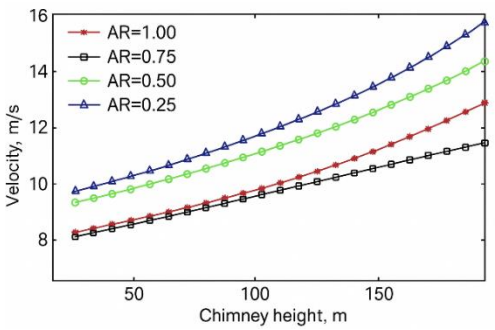

Figure 17. Estimated Velocity of the SCPP for each chimney-shape ratio examined, demonstrating the sensitivity of performance to geometric modification

4. Validation and comparison with published results

To confirm the reliability of the numerical model developed in this work, the simulation outcomes were systematically compared with existing experimental observations and peer-reviewed numerical studies on the Manzanares solar chimney prototype. These comparisons focus on key performance indicators such as air velocity at the chimney inlet and the temperature increase across the collector.

The original Manzanares solar chimney pilot plant reported airflow characteristics that serve as a primary benchmark for validation. In experimental measurements, the chimney inlet velocity was observed near 15.0 m/s under high solar radiation conditions, with a temperature rise through the collector on the order of approximately 17–20 K.

Published CFD analyses that replicated the prototype geometry and boundary conditions predicted similar performance. For instance, numerical simulations using turbulence models and radiative heat transfer approximations have obtained mean inlet velocities around 14.2 m/s and a temperature rise of roughly 18–20 K, which are close to the documented experimental figures.

Independent three-dimensional CFD investigations have also confirmed the credibility of commercially validated solvers for SCPP simulation. One recent study reproduced the Manzanares configuration for solar irradiance of 1000 W/m² and ambient temperature of 293 K, yielding maximum airspeed values near 19.36 m/s when using a divergent chimney and convergent collector geometry, with ground temperatures exceeding 360 K in the heated region.

Another numerical assessment reported that, for a standard geometry at 1000 W/m², maximum air speeds of about 14.24 m/s and cumulative temperature increase of roughly 18–20 K were achieved, demonstrating good agreement between simulations and prototype behaviour.

Table 4. Key Quantitative Comparisons (for Reference)

Source	Velocity at Chimney Inlet	Collector Temperature Rise	Notes
Experimental Manzanares	~15 m/s	~17–20 K	Prototype measurements
Prior CFD studies	14.24–19.36 m/s	~18–>20 K	Axisymmetric/3D simulations
Present study	17.49 m/s	19 K	Values fall within published range above

In the current analysis, average inlet velocities and temperature rises fall within the range spanned by these literature results under comparable boundary conditions. The present model also captures the qualitative trend of stronger airflow and larger temperature increases with higher solar radiation, in agreement with prior CFD validations. The close alignment between the simulated and published velocities and temperature patterns supports the numerical model's validity and indicates that the governing equations, turbulence closure, and

radiation treatment are producing realistic representations of the physical SCPP behaviour.

5. Conclusions

In this research, the numerical investigation carried out in this study shows how strongly the performance of a solar chimney power plant depends on the interaction between solar heating, collector geometry, and chimney design. Across the simulated radiation range of 400–1000 W/m², the system produced inlet velocities from approximately 11.8 m/s up to nearly 22.5 m/s, accompanied by temperature increases inside the collector region from 300 K to roughly 379.5 K. These changes directly translated into higher driving pressure differences and stronger buoyancy-driven airflow.

Geometry also played a decisive role. Increasing the chimney height consistently improved velocity and power output, although the improvement rate declined as the structure approached very large heights. The analysis indicated that elevations near 1900 m approach a practical upper limit, beyond which additional height yields only marginal gains. The collector radius showed a similar trend: performance improved rapidly up to about 320 m, continued to increase more slowly toward 395 m, and then levelled off as radiative and conductive losses outpaced the benefit of enlarging the collector field.

Different chimney shapes produced distinct flow characteristics. Convergent chimneys with outlet-to-inlet area ratios ranging from 0.25 to 0.75 increased flow acceleration compared with the uniform-diameter tower. The smallest tested ratio, AR = 0.25, generated the largest velocity rise through the chimney. However, this configuration shifted the peak velocity upward toward the chimney exit, suggesting that any turbine designed for such a layout would need to be positioned near the top of the structure, which introduces installation and maintenance challenges.

Limitations may be like the simulations were conducted under steady-state conditions, which do not fully capture transient effects such as diurnal solar variation, night-time cooling, or dynamic thermal storage behavior. An axisymmetric model was adopted to reduce computational cost. While suitable for ideal conditions, this approach cannot represent three-dimensional flow asymmetries, circumferential non-uniformities, or wind-induced effects. Soil was considered as a homogeneous thermal storage medium with constant properties. Variations in soil composition, moisture content, and long-term heat accumulation were not investigated.

Future studies should incorporate time-dependent simulations to evaluate system performance over full day–night cycles and seasonal variations. Extending the model to three dimensions would allow investigation of asymmetric flow patterns, crosswind effects, and structural non-uniformities. Alternative storage materials such as water, phase-change materials (PCMs), or hybrid ground–water systems can be explored to improve night-time performance.

Overall, the simulations highlight several design ranges that balance performance and practicality: collector radii up to roughly 395 m, chimney heights approaching—but not greatly exceeding—1900 m, and moderately convergent chimney profiles. These results can assist in selecting dimensions and operating strategies for future SCPP installations and provide quantitative benchmarks for further experimental and economic assessments.

Nomenclature

α	Thermal diffusivity (m²/s)
β	Thermal expansion coefficient (1/K)
g	Gravitational acceleration (m/s²)
Hch	Chimney height (m)
I	Solar radiation intensity (W/m²)
k	Turbulent kinetic energy (m²/s²)
L	Characteristic length (collector inlet height) (m)
Pt	Power output of SCPP (W)
R	Collector radius (m)
Ra	Rayleigh number
T	Air temperature (K)
Ta	Ambient temperature (K)
ΔT	Temperature difference (K)
u	Air velocity (m/s)
ε	Turbulent dissipation rate (m²/s³)
ηc	Collector efficiency
ηch	Chimney efficiency

References

[1] Dai YJ, Huang HB, Wang RZ. Case study of solar chimney power plants in northwestern regions of China. Renewable Energy. 2003;28:1295–1304. doi:10.1016/S0960-1481(02)00227-6.

[2] Pastohr H, Kornadt O, Klaus G. Numerical and analytical calculations of the temperature flow field in the upwind power plant. International Journal of Energy Research. 2004;28:495–510. doi:10.1002/er.978.
[3] Pretorius JP, Kroger DP. Critical evaluation of solar chimney power plant performance. Solar Energy. 2006;80:535–544. doi:10.22059/JSER.2019.70911.
[4] Ming T, Liu W, Pan Y, Xu G. Numerical analysis of flow and heat transfer characteristics in solar chimney power plants with energy storage layer. Energy Conversion and Management. 2008;49:2872–2879. doi:10.1016/j.enconman.2008.03.004.
[5] Ming T, et al. Numerical simulation of the solar chimney power plant systems coupled with the turbine. Renewable Energy. 2008;33:897–905. doi:10.22059/JSER.2019.70911.
[6] Xinping Z, et al. Analysis of chimney height for solar chimney power plant. Applied Thermal Engineering. 2009;29:178–185. doi:10.2298/TSCI101110017A.
[7] Lorente S, Koonsrisuk A, Bejan A. Constructal distribution of solar chimney power plants: Few large and many small. International Journal of Green Energy.
https://doi.org/10.1080/15435075.2010.529402
[8] Xu G, et al. Numerical analysis on the performance of solar chimney power plant system. Energy Conversion and Management. 2011;52:876–883.
[9] Ming T, et al. Numerical analysis on the influence of ambient cross wind on the performance of solar updraft power plant system. Renewable and Sustainable Energy Reviews. 2012;16:5567–5583. doi:10.1016/j.enconman.2010.08.014.
[10] Li J, Guo P, Wang Y. Effects of collector radius and chimney height on power output of a solar chimney power plant with turbines. Renewable Energy. 2012;47:21–28. doi:10.1016/j.renene.2012.03.018.
[11] Choi YJ, et al. Development of analytical model for solar chimney power plant with and without water storage system. Energy. 2012;112:200–207. doi:10.1016/j.energy.2016.06.023.
[12] Fasel HF, et al. CFD analysis for solar chimney power plants. Solar Energy. 2013;98:12–22. doi:10.1016/j.solener.2013.08.029.
[13] Cao F, et al. Design and simulation of solar chimney power plant with TRNSYS. Solar Energy. 2013;98:23–33. doi:10.1016/j.solener.2013.05.022.
[14] Ming T, et al. Numerical analysis on the solar updraft power plant system with a blockage. Solar Energy. 2013;98:58–69. doi:10.1016/j.solener.2013.02.027.
[15] Koonsrisuk A, Chitsomboon T. Effects of flow area changes on the potential of solar chimney power plants. Energy. 2013;51:400–406. doi:10.1016/j.energy.2012.12.051.
[16] Koonsrisuk A. Comparison of conventional solar chimney power plants and sloped solar chimney power plants using second law analysis. Solar Energy. 2013;98:78–84. doi:10.1016/j.solener.2013.02.037.
[17] Patel SK, Prasad DD, Ahmed MR. Computational studies on the effect of geometric parameters on the performance of a SCPP. Energy Conversion and Management. 2014;77:424–431. doi:10.1016/j.enconman.2013.09.056.
[18] Okada S, Uchida T, Karasudani T. Improvement in solar chimney power generation by using a diffuser tower. Journal of Solar Energy Engineering. 2015;137:031009. doi:10.1115/1.4029377.
[19] Gholamalizadeh MT, Wei L, Guoliang X. Analytical and numerical investigation of the solar chimney power plant systems. International Journal of Energy Research. 2006;30:861–873. doi:10.1002/er.1191.
[20] Cottam PJ, et al. Effect of canopy profile on solar thermal chimney performance. Solar Energy. 2016;129:286–296.
doi:10.1016/j.solener.2016.01.052.
[21] Huang MH, et al. A two-dimensional simulation method of the solar chimney power plant with a new radiation model for the collector. Heat and Mass Transfer. 2017;85:100–106. doi:10.1016/j.icheatmasstransfer.2017.04.014.
[22] Semai H, Bouhdjar A, Larbi S. Canopy slope effect on the performance of the solar chimney power plant. International Journal of Green Energy. 2017;14:229–238.
doi:10.1080/15435075.2016.1253580.
[23] Rabehi A, et al. CFD analysis on the performance of a solar chimney power plant system: Case study in Algeria. International Journal of Green Energy. 2017;14:971–972. doi:10.1080/15435075.2017.1339043.
[24] Zhou X, Xu Y, Hou Y. Effect of flow area to fluid power and turbine pressure drop factor of solar chimney power plant. Journal of Solar Energy Engineering. 2017;139:041012. doi:10.1115/1.4036774.
[25] Hu YCD, Chan CY. Impact of the geometry of divergent chimneys on the power output of a solar chimney power plant. Energy. 2017;16:31904. doi:10.1016/j.energy.2016.12.098.

[26] Xu Y, Zhou X. Performance of divergent-chimney solar power plants. Solar Energy. 2018;170:379–387. doi:10.1016/j.solener.2018.05.068.
[27] Haff W. Part II: Preliminary test results from the Manzanares pilot plant. International Journal of Solar Energy. 1984;2:141–161. doi:10.1080/01425918408909921.
[28] Cuce PM, Saxena A, Cuce E, Kontoleon KJ, Oztekin EK, Shaik S, Guo S. Thermal and energy analysis of a novel solar updraft tower design with divergent chimney and convergent collector concept: CFD analysis with experimental validation. Int J Low-Carbon Technol. 2024;19:714–722. https://doi.org/10.1093/ijlct/ctad152
[29] Benettayeb Y, Benbouali A, Tahri T, Cuce E. Performance analysis of the impact of sloped absorber dimensions on the performance of solar chimney power plants. J Therm Anal Calorim. 2025;150:9561–9571. https://doi.org/10.1007/s10973-025-14307-4
[30] Danook SH, Al-bonsrulah HAZ, Hashim I, Veeman D. CFD simulation of a 3D solar chimney integrated with an axial turbine for power generation. Energies. 2021;14:5771. https://doi.org/10.3390/en14185771
[31] Fertahi SED, Rehman S, Lahrech K, Samaouali A, Arbaoui A, Kadiri I, Agounoun R. A review of comprehensive guidelines for CFD validation in solar chimney power plants: methodology and Manzanares prototype case study. Fluids. 2024;9:251. https://doi.org/10.3390/fluids9110251
[32] Cuce PM, Cuce E, Omer S, Riffat S. Solar chimney power plant with integrated waste heat source on the ground: a numerical and statistical research with experimental validation. Int J Low-Carbon Technol. 2025;20:1272–1282. https://doi.org/10.1093/ijlct/ctaf077